Concept development and construction of a high-precision handling and cutting system for the automation of battery cell production

Berk Gökoglu
berkgokoglu@gmail.com

Instituto Superior Tecnico, Universidade de Lisboa, Portugal
May 2019

Abstract

In the current economy, vehicle purchasing decisions are driven by vehicle range, charging speed, cost and above all safety. All of these attributes are linked strongly with battery production technologies. In order to fulfill the performance requirements, the lithium-ion battery assembly should be completed cautiously. Besides, battery production contributes to over 40% of the vehicle battery costs. Improving the lithium-ion pouch cell production speed is the key objective of this dissertation. The scope includes the processes between the calendered material roll and die-punched single sheets. To make improvements in this setup, web handling mechanics were investigated. Using state of the art and experimental outcomes of the current studies on web converting applications, as well as electrode web processing, a series of experiments were designed. The experiments aimed to verify whether these principles would apply for the cathode and anode of the lithium-ion cells. Tension, velocity, misalignment angle, and web span seem to have a strong correlation to the instabilities of the web. In regard to literature and experimental analysis, there is a compromise between product quality and manufacturing speed. Given the theoretical and empirical results, two alternative designs were developed to make improvements on the present pouch cell manufacturing process. These designs feature significant improvements in web stability and cycle time. Moreover, the linear motion identified as a bottleneck of the electrode processing unit was replaced with alternative approaches to improve the lead times substantially. Consequently, the conceptualized designs were compared on a theoretical frame. A plausible design was proposed as a result of this comparison. With the featured proposal, the cycle time is presumably improved by 38.3% in contrast to the reference technology.

Keywords : Lithium-ion, Production Technologies, Pouch Cells, Single sheet stacking, Electrode web

1. Introduction

Commercial availability of lithium-ion batteries is one of the great challenges facing the automotive industry. To address these challenges, the lithium-ion battery retail prices play a prominent role. Most of the research and development has focused on a selection of abundant materials. Manufacturing processes, however, contribute to about 47% of the overall battery costs, which is often overlooked [1].

The aim of this study is to improve the production speed for single-sheet stacking of lithium-ion pouch cells and thereby reducing the unit costs of the vehicle batteries. The objectives of this project were established within the framework of the "Competence E" project, which was performed at Karlsruhe Institute of Technology Institute of Production Technologies (KIT wbk). "Competence E" was launched with the purpose of developing a cost-effective, industry-applicable new generation lithium-ion batteries as well as the production system for e-mobility applications [2].

Handling limp electrode material and long cycle times due to the linear movement were the challenges that created a basis for this work. Despite the efforts on increasing productivity of lithium-ion manufacturing systems, the handling stability of the limp electrode sheets is not yet fully attained [3;4;5]. It is, therefore, worthwhile to shed light on this aspect of the process to improve productivity and operational stability. In this context, the literature on web stability along with web converting principles and technologies was reviewed to gain insights that created the baseline for the experiments.

The scope of this study encompasses the formation processes of single sheets utilizing calendered electrode rolls.

1.1. Single Sheet Stacking Developed in KIT

The processes described in this section refer to the single sheet stacking unit developed in KIT wbk. The setup is shown in **Error! Reference source not found.**. Initially, using a servo motor driven mandrel (marked as '**1**'), calendered electrode rolls are unwrapped and the web is transported through a dancer roll system ('**2**'). The dancer roll is attached to a cylinder which is fed a tension setpoint. Change in tension presses the dancer roll and counteracts the cylinder pressure. The dancer roll moves until the pressure can balance the web tension pushing the roll in the opposite direction. The passive dancer system naturally adjusts the position of the dancer.

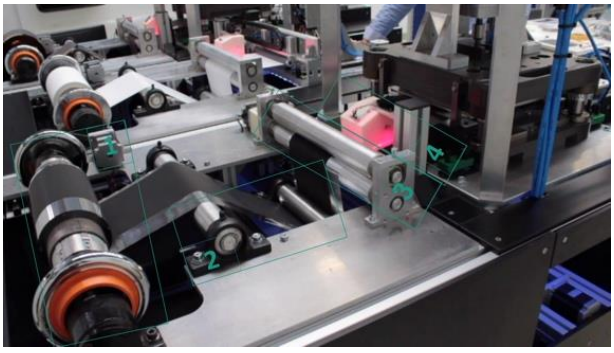

Figure 1: Single sheet stacking unit at wbk KIT.

Next, the nip roll pair ('3') translates the web 90 degrees towards the die-cutting unit. The position sensor ('4') measures the edge position of the active material. In case a precision error is present, the unwinding assembly is mounted on a guide stand which can be laterally controlled with another servo motor coupled with rack and pinion assembly. This mechanism provides clean, precisely cut electrode sheets. With the help of a vacuum gripper which is transported in a linear motion, the web is fetched and transported past the die cutting equipment. Then, the electrode strip is cut into a single sheet. The single sheet is moved to the stacking compartment with the help of another vacuum gripper. The residual material is removed as the gripper fetches the end of the electrode.

Furthermore, the separator is also processed similarly but is cut with a sharp blade instead of die cutting equipment. The single sheets are then stacked with the help of a pick and place assembly. The stacking procedure is repeated until the desired cell capacity is reached. [2] However, these final steps are out of scope for this study.

1.2. IRTM Approach

Imaginary Resistive Tension Member (IRTM) allows a simplified approach to understand the movement of the web with respect to the rolls. The entire web is virtually a network of vertical and horizontal strings aligned one after another and mechanically transmits the loads consecutively to the next string. The strings are called resistive tension members [6]. When the resistive tension member approaches the roll with a certain angle, the tension breaks down into two components: one perpendicular and another parallel to the roll axis. The parallel component is shown as F_{st} in Figure 2, is called stabilizing force, resembling the force applied on the tension member that shifts the web such that it approaches the web perpendicular to the roll. This principle is called web perpendicularity[7].

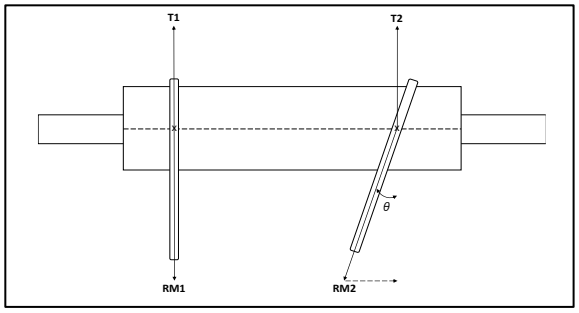

Figure 2: Illustration of IRTM approach[6]

1.3. Shelton's Beam Theory Approach

Euler-Bernoulli beam theory was implemented by Shelton to conceptualize the loads acting on the web and the lateral motion of the web due to misalignment between the rolls transporting the web.

The following assumptions made this theory applicable:

- All deflections are relatively small.
- Web camber and uneven surfaces are negligible.
- The web has a homogenous and uniform structure and is free of local imperfections.
- Shear deflection is trivial, the web that enters the web perpendicular to the roll axis remains perpendicular.

Solving the beam theory equation with respect to critical misalignment angle the aggregate function is as follows:

$$\theta_{L,crit} = \frac{Kw}{6}\frac{\cosh(KL) - 1}{\sinh(KL)} \quad (1)$$

where $K = T/EI$ and $I = \frac{tw^3}{12}$. $E, \theta, L, t,$ and w stand for Young's modulus, misalignment angle, length, thickness, and width, respectively. According to Shelton's static behavior, the critical angle of misalignment depends on Young's modulus, the moment of inertia, width, length and tension applied on the web [8].

1.4. Web Handling Problems

Wrinkle formation is the most common problem in web handling applications since these defects degrade the web quality, result in machine downtimes and material loss. Identifying potential causes of wrinkling and intervening against permanent wrinkles improves the performance of the web handling equipment [9]. Typical wrinkle forming conditions are associated with errors such as roll misalignment, web-treatment problems and the imperfections on the roll geometry. These problems usually result in wrinkles reappear in the same location. If the location of the wrinkles is unstable, then the problem is presumably span or time-dependent. These type of formations can be a result of factors such as the inaccurate tension control, uneven or cambered web surfaces. [6]

Delamination is a problem associated particularly with lithium-ion electrode handling. Strong adhesion between the active material and current collector is essential to prevent rapid ageing of the cell. Delamination indicates loss of electrical contact between the active material and current collector, which induces internal impedance and triggers the ageing process. Delamination can occur either during the operation of the battery or during the electrode handling due to excessive bending loads. [10]

Furthermore, relative motion between the roll and web can result in scratches on the web surface. Relative motion forms a zone within the wrapped surface that has raised tension between web entering the roll until it leaves the roll. This zone is known as the creep zone due to elongation resulting from tension differences. If the creep zone grows beyond the plastic deformation limit of the material, the scratches appear on the surface of the web [6].

2. Methodology

The aforementioned processes and research allowed to define potentially critical parameters that have a significant effect on web stability and critical operation velocity. Experiments were designed such that the effect of these parameters can be examined. After these experiments were carried out, the system was designed to eliminate the cause of instabilities evaluated during the experiments. After the design proposals were presented, comparing the proposals with the reference setup according to the key performance indicators, the optimal design was designated.

In order to validate if the reviewed literature agrees with the experiments on the material, the anode, cathode, as well as aluminum foil were tested for isotropy, Young's modulus, yield force, and maximum admissible force. The elementary beam theory applies to isotropic webs [8]. The web isotropy was tested by taking an equal number of samples from the web in both horizontal and vertical directions.

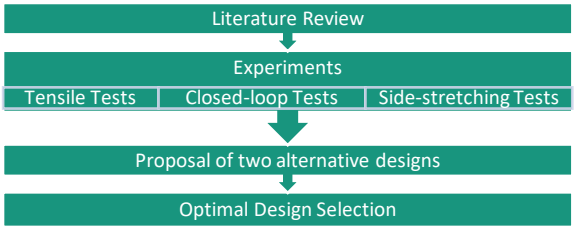

Figure 3: Structure of the study.

Young's modulus should be applied to the aggregate function yielded by Sheldon. Yield force and maximum admissible force is recorded to quantify the limits of the electrode material. The tests were carried out using Zwick-Roell ZwickiLine material testing equipment.

Aluminum and cathode web were wrapped around a driven and an idle roll. Ends of the web were fixed onto each other by adhesive tape to form a loop enclosure, as seen in Figure 4. Such setup was used to emulate the motion of the web driven by the roller until it reached the die cutting tool on the reference handling system. This test bench allows to adjust the following parameters: web velocity, web tension, misalignment angle, and web span.

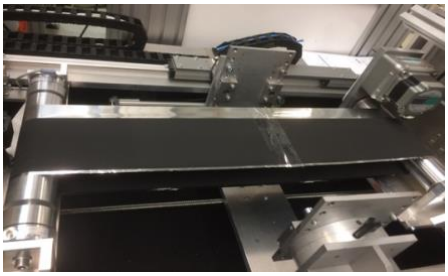

Figure 4: Closed-loop Setup with cathode web.

The experiment was performed with different web span, tension, velocity, misalignment angles. The load cell on the idle roll measured the tension variations on the web instantaneously as a camera mounted onto the setup filmed each experiment. With such data gathering, the effects of each parameter on web stability and critical velocity will be examined. Also, experimental results were correlated with the literature research to verify if the electrode web material would respond similarly.

It was foreseen that counteracting the shear forces would eliminate folds and straighten the web in the lateral direction. Elimination of these folds would imply better stability enabling higher operation speeds. To validate the accuracy of this hypothesis, side clamp design was proposed and evaluated in the side-stretching setup shown in Figure 5.

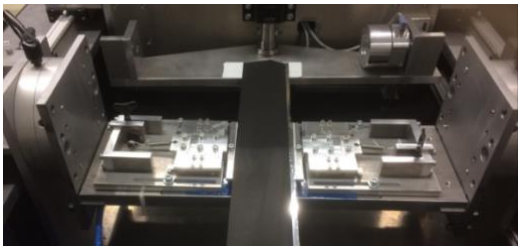

Figure 5: Side Stretching Setup

A rail moves the module in the lateral direction and thus allows the stretching. The rail plate meshes with a guide mechanism, and their coefficient of friction is in the range of 0.04 and 0.08. This connection constraint all degrees of freedom except that in the lateral direction. Tension spring is attached to the rail. A bass guitar tuner is used to adjust the position of the spring. The spring is connected to the tuner via a fabric string which transmits the tension. The tension range foreseen for each spring is $0 - 25\ N$. Rotating the bass tuner handle in the clockwise direction, the string tension rises which pulls the web outwards.

3. Results

3.1. Stress-Strain Tests

The experiments were carried out on pure aluminum, cathode, and anode samples. Stress-strain curves of the aluminum, cathode and anode are illustrated in Figure 6, Figure 7 and Figure 8, accordingly. Pure copper sample tests were not performed. The reasons for such setback are discussed in Section **Error! Reference source not found.**.

Four pure aluminum samples on each direction were placed on the tensile testing machine. The stress-strain graph for these tests is shown in Figure 6. The terms "long " and "lat" indicate the cutting direction of the samples. The average Young's Moduli are 27.8 GPa and 32.6 GPa for lateral and longitudinal samples. Despite the similarity between the stress-strain graph for samples in different directions, the isotropy of the aluminum foil is controversial.

Five samples of cathode web samples are tested in each cutting direction. The samples were 3 mm wide, 14.5 mm long and 116 μm thick. As the average Young's moduli were 6.2 GPa and 6.3 GPa for lateral and longitudinal samples, accordingly. Hence, the cathode is presumably isotropic. Figure 7 shows the similarity between different samples which is in agreement with this statement.

Four lateral and five longitudinal anode samples were subjected to the tensile test. The samples were 145 μm thick, the same width and length as the cathode samples. 0.47 GPa and 0.45 GPa were the average Young moduli of the lateral and longitudinal samples, respectively. A difference of 0.02 GPa points to isotropic behavior which also shows a similar view in Figure 8.

The average yield force for pure aluminum and cathode foils were 76 N and 75 N, accordingly. On the other hand, maximum admissible and yield forces were 98.7 N and 76 N for aluminum, and 96.2 N, 76.8 N for cathode samples, respectively.

The similarity of the yield strength and admissible force signifies that the double-sided graphite coating does not influence the yield stress. The anode has yield and admissible force of $104.8\,GPa$ and $124.36\,GPa$, accordingly. In contrast to the cathode, the anode has a higher yield and a maximum admissible force.

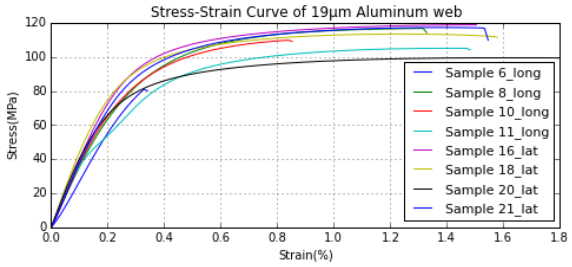

Figure 6: Tensile analysis of aluminum samples

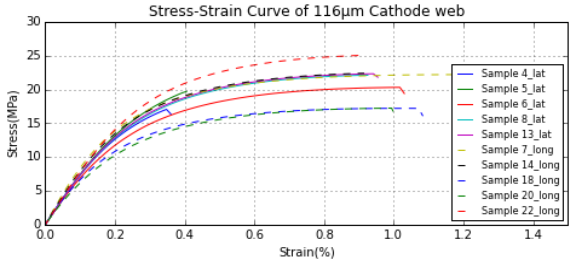

Figure 7: Tensile analysis of cathode samples

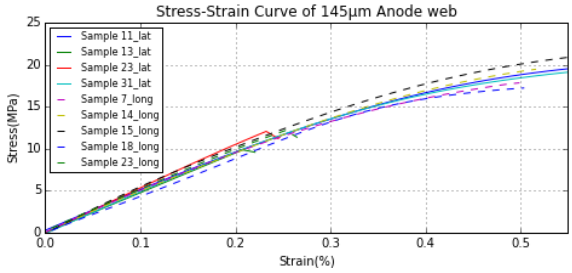

Figure 8: Tensile analysis of anode samples

3.2. Closed-loop Experiments

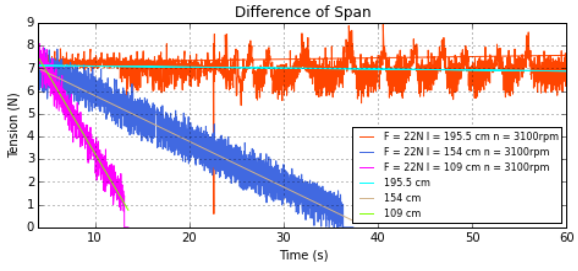

Figure 9: Effects of web span with IRTM approach

The effects of the web span were tested on aluminum and cathode. It was, however, reasonable to visually interpret the results of a fabric string on the closed-loop setup as this setup would agree with IRTM approach. As the string represents the single string member of an electrode web, the effects are clearly distinguishable. The results are shown in Figure 9.

The tension on the y-axis resembles the tension measurement performed by the load cell. The orange, blue and magenta plots represent the measurements of the strings with $109\,cm$, $154\,cm$, and $195.5\,cm$ total length. On the other hand, cyan, light brown and light green lines are linear regression fits of the corresponding plots. With shorter span lengths, shear forces arise causing the strand to shift further away from the load cell. This principle explains tension slope change as the web gets shorter. This behavior conforms Shelton's theory. The correlation of lateral movement and web span is shown in Figure 10.

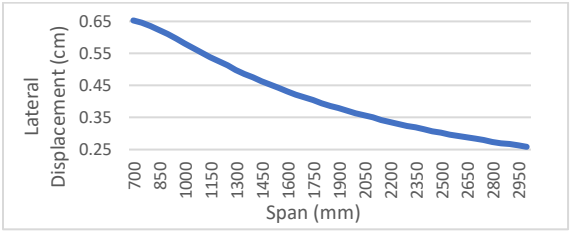

Figure 10: Relation between lateral displacement and span

Aluminum foil with a thickness of $19\,\mu m$ was introduced into the closed-loop setup. Aluminum web with a total loop span of $158\,cm$ was tested at a motor speed of $300\,rpm$. Web tension values were $29\,N$, $69\,N$ and $90\,N$.

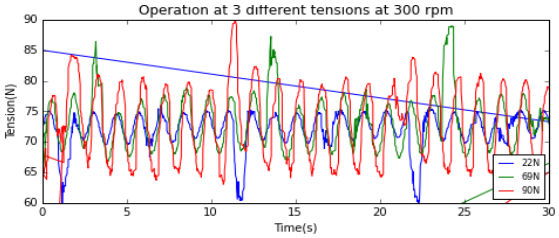

Figure 11: Aluminum web under 3 different tensions

Normally it was expected that an undulating motion of the web would result in larger tension variations due to low tension operation, while holding the desired web tension higher would result in smaller undulating motion resulting in lower intensity tension variations [11]. However, this experiment suggests otherwise. These experiments indicate that it is preferable to operate the web at lower tensions. The web with high tension causes large tension peaks and also a larger range of tension fluctuations.

Figure 12: Cathode web tension profile at different speeds

Figure 12 illustrates the comparison of the cathode with different operating velocities. Higher speed intensifies rapid peaks in the tension profile. These peaks should be accounted for especially at high web tensions, as the peaks can damage or even break the web. These peaks appear to be periodic, which could be an indication of a specific position of the tissue causing the peaks.

Tension profiles of aluminum and cathode webs were investigated at $100\,rpm$ engine speed. The result is illustrated in Figure 13. Both samples were carried out under the longitudinal stress of $68.5\,N$. The average tension was around $25\,N$ as the tension profile was measured with only one of the load cells.

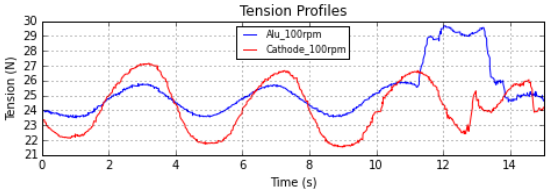

Figure 13: Aluminum and Cathode webs at 100 rpm

There are two major differences in the tension profiles. Looking into the time intervals between $0-10\,s$ tension fluctuation was roughly $2.1\,N$ and $4.9\,N$ for aluminum and cathode samples, respectively. Secondly, there was a tension peak for one sample between 11.5 s and 13.5 s and a tension trough for the other. The adhesive tape altered the web thickness at this location causing these peak and troughs. Aluminum web has a larger peak in contrast to the cathode web. This difference is likely due to the stiffness difference between these materials.

Stiffness ratio of the was larger by a factor of 44.58. Thus, the stiffness ratio is directly proportional to the tension variation and inversely proportional to tension peaks. In other words, the coating material causes a large increase of stiffness ratio, which results in a larger rise in tension variations and fewer tension peaks.

Figure 14 illustrates a comparison of misalignment angle operating the aluminum foil at an engine speed of $100\,rpm$ and a total tension of $68\,N$. The measurement here was performed only by the left load cell. The shift in tension is a result of the web moving further away from the load cell. Hence, misalignment influences the lateral movement significantly. The misalignment angle should be kept to a minimum as even a slight misalignment results with imprecisely cut electrode sheets due to lateral movement.

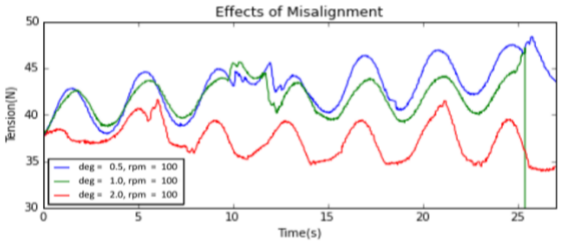

Figure 14: Single side load cell readings at 0.5º , 1º and 2º.

An aluminum web with a taut center and a single-sided, baggy edge were accidentally developed as a result of inadequate adhesive tape application. The web was conducted with tension $22\,N$ at a motor speed of $100\,rpm$, and the video was recorded at a rate of $120\,fps$. Reviewing the video at the rate of $24\,fps$ improved the ability to capture details regarding the motion of the sample. Figure 15 illustrates the instant the web surface with adhesive tape was in contact with the roller (left) and after this surface leaves the roller (right).

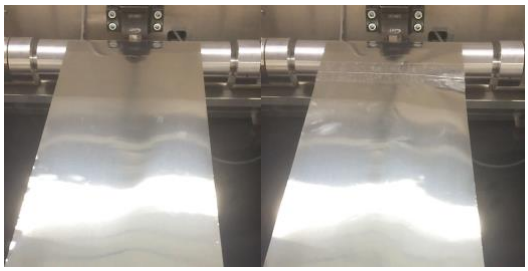

Figure 15: Web with a baggy edge

The additional degree of freedom due to baggy edge enabled the formation of a tension difference through the baggy portion of the web causing undulating motion. If this undulating motion exceeds the maximum strain the web can handle, local plastic deformations occur on the surface of the web resulting in permanent marks on the web.

At higher speeds, the air film between the roller and web is thicker. This results in trapped air bubbles which cause localized pressure fluctuations leading to dents on the material surface. On the other hand, similar dents can also result from roll surface imperfections. Figure 16 shows indentations due to air entrainment at high-speed operation. These dents, however, were not present on the cathode web at the same operation speed. A likely explanation could be that active material layers on both sides have more resistance against the localized pressures.

Figure 16: Indentations on the Al surface due to 1100 rpm operation

3.3. Side-stretching Experiments

Externally applied shear forces remove the longitudinal wrinkles when applied with the right intensity. Such a conclusion was derived from the evaluation based on the graph illustrated in Figure 17. The longitudinal tension applied on the sample, and lateral tension applied to remove the fold formed by the assembly shown in Figure 5.

The anode was tested under shorter web spans. When long anode sample was tested with the same setup, folds did not sustain to reach the side stretching assembly. The cathode and aluminum samples were tested with similar spans which were longer than the anode sample. Aluminum had much lower bending stiffness in contrast to the cathode material. It is thus harder to generate folds on the cathode web. Cathode samples required higher web tensions to generate a similar longitudinal fold. Thus the results of the side-stretching experiments on different web materials should be evaluated separately.

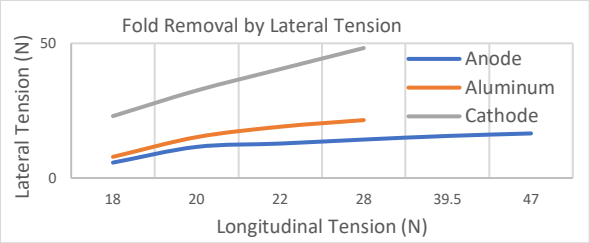

Figure 17: Lateral loads to remove longitudinal wrinkles

Side stretching assembly enables a great degree of controllability of the folds. Different electrode materials require a different amount of tension to spread out the folds. Adjustable spreading allows the flexibility to deal with a range of different type of folds on the electrode web. Therefore, this type of setup was seen as a web spreading solution for a variety of web spreading applications.

4. Solutions and Conclusions

4.1. Contactless Electrode Transport

Concave radial air bearing ('**1**') allows the web to shift in both lateral and longitudinal directions eliminating the need of an additional web guide adjusting the air flow. The air bearing is used in combination with the Air Turn rolls[12]. This combination is the main feature of this system design as it allows contactless web transport, which significantly improves stability and cycle time.

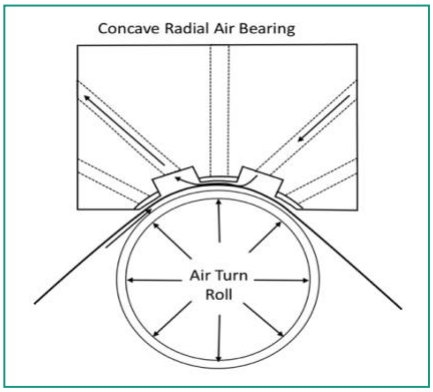

Figure 18: Air Turn roll and concave radial air bearing[12]

The porous structure of the Air Turn rolls enables uniform air flow. Uniform flow is essential for stability and precise control of the distance between roll and web. The Air Turn roller replaces the aluminum driven, idle and dancer rolls on the reference design.

The airflow that strikes the web surface follows the surface and leaves the web eventually inducing a self-spreading effect. This effect ensures that the web is kept taut in both the lateral and longitudinal directions as it passes through the rolls allowing additional operation stability. Thanks to the contact-free operation, the acceleration and deceleration cause fewer disturbances during start-up and cut-off. This can be explained by the elimination of inertial forces.

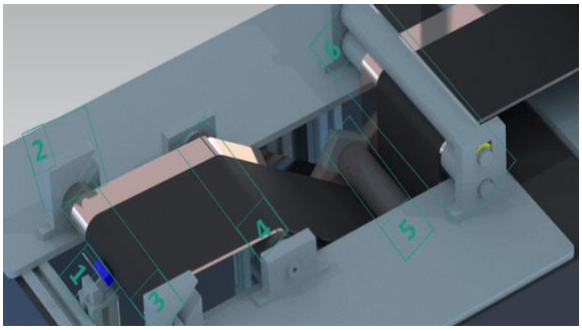

Figure 19: Contactless transport design unwinding assembly

Support plate design of the driven roll ('**2**') features easy mounting and dismounting allowing quick material roll changes. This feature replaces the function of the safety chuck on the reference design. When the material roll is to be replaced, the driven roll can simply be removed through the channel guide. The channel guide is inclined so that the roller is locked in place unless the roller is pushed in the machine direction and lifted at the same time. This design feature facilitates safe operation and practical removal of the material roll without additional tools.

To minimize tension fluctuations, support plates of the dancer roll ('**5**') are attached to a pneumatic cylinder which is adjusted via an encoder using the output of the dancer position sensor. To keep the web taut when the die-cutting tool is penetrating the web, the aluminum nip roll pair ('**6**') is preserved as the existing design.

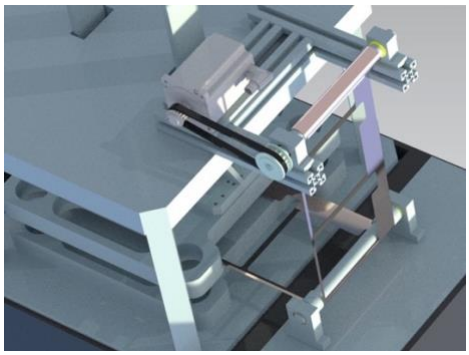

Figure 20: Web transport after the die-cutting assembly

Linear motion of the gripper is eliminated by replacing it with an aluminum idler roll. The discontinuity of the residual material is avoided by improving traction through the design shown in Figure 20. The surface is designed such that roll contacts the web only at the points where there is residual material. This roll is followed by a driven aluminum roll which is used to wind up the residue. Driven roll is connected to a servo motor through a gear-belt pair. Coordination of the servo motor and the radial concave air bearing is necessary; thus an additional encoder is required.

4.2. Second Design

The lateral position should be precisely handled on the single sheet stacking. The electrode sheets should be cut precisely to obtain standard quality and safety. The linear guide is located at the ends of the unwinding assembly. The carriage supporting the frame provides lateral positioning. Linear guide rail features low-friction movement and constrains the carriage movement to one axis. The motion is obtained through a stepper motor. The torque is then transmitted through a coupling between the stepper motor and shaft-hub connection that drives a ball-screw pair. A ball nut is attached to the bottom of the carriage. When the stepper motor rotates the screw shaft, the ball nut starts moving. The moving direction is defined by the rotational direction of the stepper motor.

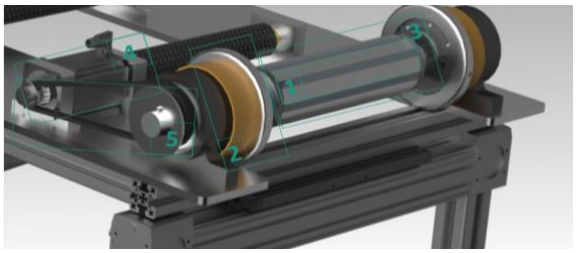

Figure 21: Unwinding roll and drive

Unwinding mechanism is similar to the reference system described in 0. As shown in Figure 21, the longitudinal traction bars (‘**1**’) lock up the material roll as it begins to rotate. The material roll can be removed easily by sliding it off in the lateral direction. The safety chuck (‘**2**’) enables quick material roll changes. This component moved sideways with a push by hand releasing the upper part of the square key geometry. The roll is now no longer constrained in the x-direction (opposite of the direction of gravity). The unwinder roll (‘**3**’) can then be removed by simply raising it. Once the new material roll is placed onto the unwinder roll, it can be relocked by clicking the safety chuck back into its initial position. A stepper motor (‘**4**’) drives the roll. Torque is transmitted via gear-belt pair (‘**5**’).

All of the following parts described are shown in Figure 22. It is desirable to use carbon fiber roll on idler rolls (‘**2**’), instead of the aluminum roll as it features improved stability and better acceleration. There are two main reasons for this selection. First, aluminum rolls can contaminate the electrode surface. The carbon fiber roll is less risky, since the carbon fiber coating is durable, and the material worn out is not electrically conductive. Secondly, the rotational inertia of the aluminum rolls may undulate the web during the acceleration and deceleration of the rolls. Carbon fibre rolls have less inertial effects as they are lightweight. The dancer arrangement (‘**3**’) is similar to that described in the contactless electrode transport design with the exception of the roll type.

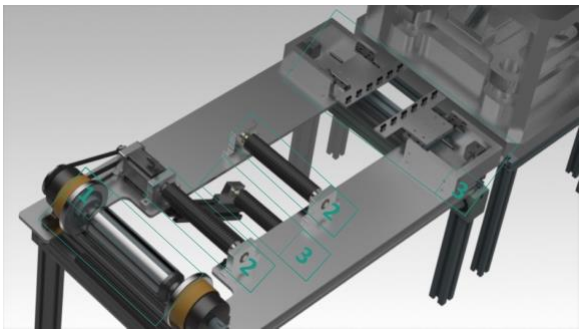

Figure 22: Unwinding Assembly

Carbon fibre roll is also used for the dancer eliminating the requirement of complicated dancer control. To minimize the folds induced by shear stresses, a considerable amount of space is left between the idler roll after the dancer roll and the side stretching assembly. As concluded in 3.2, longer span recuperates web stability. The adjustable vacuum side stretching assembly removes the remaining folds.

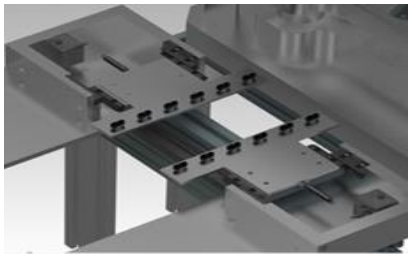

Figure 23: Vacuum side stretching assembly

Side stretching assembly (‘**3**’) is activated as the web stops moving. Such a response allows clamping force while the die-cutting assembly is penetrating the web. This simultaneous action increases utilization; no additional time is required for enhanced stability and wrinkle removal.

The side stretching assembly design is illustrated in Figure 23. Gripping is activated through six flat suction cups located under both sides of the web. Stepper motors located on both sides start pulling on a metal string ensuring the wrinkles are evened out. Having separate motors on the sides allow lateral position adjustment as well as advanced wrinkle control over the web. A metal string is connected to a spring which allows precise measurement of the forces applied on the web by measuring the elongation of the spring. Pulling forces exerted on the spring moves the guide plate through a low friction linear guides. As the die-cutting is completed, a controller interrupts the vacuum supply of the suction pads so the web can start moving again in the machine direction.

After the electrode sheet is cut the web starts moving again. The residual material is drawn by a vacuum roll (‘**1**’) and winded by a wind-up roll (‘**2**’) shown in Figure 24. The vacuum roll was selected for two main purposes. The residual material is too delicate to handle with an aluminum roll. Any web discontinuation results in increased dead time reducing the productivity of the production.

Table 1: Comparison of contactless electrode transport, the second and the reference design

Concept Designs	Percentage (%)	Contactless Transport		Second Design		Single Sheet Stacking Unit at wbk	
		Points	Value	Points	Value	Points	Value
Stability	15	5	75	3	45	2	30
Speed	15	4	60	3	45	2	30
Material Quality	14	5	70	4	56	3	42
Process Reliability	13	3	39	3	39	5	65
Contamination	10	5	50	4	40	3	30
Costs	10	2	20	3	30	4	40
Lifetime	9	4	36	3	27	3	27
Maintenance	8	4	32	3	24	3	24
Mounting	6	5	30	4	24	4	24
Total	100	412		330		312	

The vacuum provides a uniform negative pressure around the web, avoiding potential tears. Moreover, even if the web is torn longitudinally, since a vacuum uniformly across the web, the discontinuity could be prevented. Secondly, vacuum roll and the side clamp mechanism secures a taut web so that the die mold can go through the web with precise positioning. A stepper motor ('3') drives windup roll. Torque is transmitted through a gear belt pair. Rotation pulls the web from the vacuum roll and collects it around the windup roll. Windup roll diameter is much less than the other rolls to maximize the collection of material residue without needing to dismount the roll.

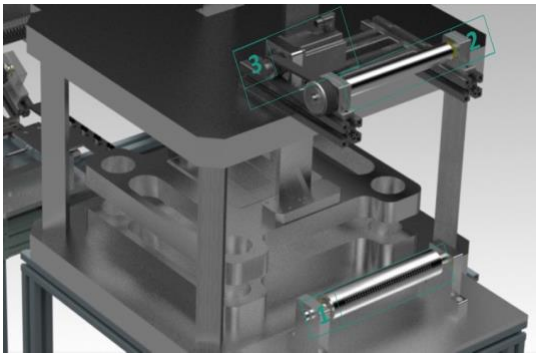

Figure 24: Vacuum gripper roll and the winding roll

4.3. Final Selection and Process Parameter Proposals

Table 1 shows a comparison of the two design proposals and single sheet stacking unit at KIT wbk. In this section, the single sheet stacking unit at wbk is referred to as the current system. Stability and speed are the primary key performance indicators of this work. Obtaining improved results of these parameters makes the production process faster and cost-efficient.

Improving process speed without satisfying material quality standards is necessary for lithium-ion battery production. Electrode sheets are required to have a preserved surface quality free of scratches, wrinkles, and loose-particles. Electrode web transport should operate without stopping due to any discontinuity or other process errors. This factor is considered under process reliability. Furthermore, contamination is a primary concern for lithium-ion batteries. Particularly for safety reasons, electrode webs should be free of any sharp pieces, burr and water particles.

Cost and lifetime of the material are considered together. A long lifetime of a product can make up for the cost differences. The frequency of the maintenance required and practicality of mounting is considered as these factors affect the downtime of the production.

Contactless transport delivered through Air Turn rolls and radial concave air bearing, material conveyed to the die-cutting assembly offers excellent stability. Airflow used to lift and adjust the web has a self-spreading effect. This effect hinders potential fold formations. Friction-free lateral shift minimizes the potential of localized shear stresses. Second design also has improved stability as the lightweight carbon fibre rolls reduce inertial forces exerted on the web. In addition, the side stretching assembly features active wrinkle removal. However, since there is still contact between the web and carbon fibre rollers, stability is still an challenge due to friction. Furthermore, a smooth roll surface may cause web slip causing complications. The current system has stability problems. These problems are associated with the short span between the rollers, sizeable inertial forces particularly during acceleration and deceleration and lack of a spreading solution.

Using the pressure differences, an air bearing can adjust the bearing both laterally and longitudinally. Contactless transport enables friction-free transport of the medium. Such transport enables high-speed operation. Web speed is rather limited on the other two designs. Carbon fibre has a slightly better speed performance since it is lighter than aluminum rolls. This reduces the impact of inertial forces. Cycle time of the current system is limited by design due to stability problems and the time required to complete the linear movement of the gripper.

Both of the proposed designs feature an acceptable electrode sheet quality. This is obtained by optimizing the process parameters as well as adjusting the design aiming for the stability improvements. Contactless web transport, minimizes the possibility of scratches as the only section which has contact with the web is the nip-roller. The contactless solution has passive spreading while the second design has an active spreading. Spreading also implies a considerable quality improvement on the electrode sheets. Fold formations are less likely to occur in the presence of spreading. Quality of the current solution is also acceptable but has room for improvement.

Process reliability is uncertain for both of the designs as both require airflow to fulfill specific functions. Obtaining a reliable operation is complicated and requires a substantial amount of testing before the designs can be implemented into commercial use. Besides, the contactless transport of the electrode web is not yet tested. Thus, it is not yet clear whether it can be transported flawlessly by the airflow. The current design, however, is proven to be reliable and functional despite the stability problem and non-ideal process cycle times.

Contactless transport has no risk of wear over time as it provides a contamination-free environment. The compressed air provided, however, should be filtered before it is fed to the radial air bearing and the Air Turn rolls. The second design will also not have much wear since the coating applied to the carbon fibre rolls are durable. Aluminum rolls fulfill web transport in the current system. Wear and material chip-off can build-up in the environment over time. This poses a risk for the lithium-ion cells. Particularly, sharp particles may puncture the surface of the separator as the cell is assembled and compressed into pack form.

The second design is inexpensive in comparison to contactless transport. The Air Turn and radial concave air bearing technology involves complicated design and materials. Formation of an evenly distributed network of pores on both of these structures requires complex manufacturing solutions. On the other hand, carbon fibre is also costly in contrast to the conventional aluminum rolls. Except for the custom-designed gripper, the current solution is composed of widely available standard components. It is thus a low-cost system.

Friction and wear-free operation improve the lifetime of the contactless transport design substantially. The second design is also durable but still requires maintenance. Web transport is obtained through mechanical movement on both the second design and current system. This requires periodic lubrication and maintenance of all of the bearings or replacements.

Mounting components of the second and current designs require extensive effort. Both designs rely on complete displacement guide that should be mounted onto the base plate of the entire unwinding assembly. In contrast, components of the contactless transport design can be dismounted separately. Besides, the system does not require additional components for lateral transport. The concave radial air bearing is able to control the web both in lateral and longitudinal directions. Besides, mounting of this component is much less complicated in contrast to the linear guide rail used on both the second and current designs.

As a result, both contactless transport design and the second design deliver improved overall attribute performance in contrast to the reference system. Despite high-cost components, the contactless web transport enables improved stability and speed without trading off for material quality. Such improvement is realizable through friction free-web transport, passive spreading, continuous collection of residual material instead of linear movement through grippers.

Besides the design proposals, improvements on various process parameters are necessary. The result of the experiments discussed in 3.2 implied several process adjustments. These adjustments improve the productivity of the manufacturing process and product quality. The web tension, speed, stiffness, misalignment angle, and velocity has a considerable influence on the electrode handling.

The cathode web showed more stable behavior at $22\,N$ in contrast to operating tension of $69\,N$ and $90\,N$. This behavior holds for web operation with motor speeds until $900\,rpm$. It is thus favorable to operate the web at lower tensions unless the motor speed exceeds $900\,rpm$. However, the web tension has a minimum limit. Beyond this limit, the web is not taut enough. Bagginess results in the undulating web through the operation. If the web is extensively undulated, plastic deformations on the web surface reduce the material quality.

On the other hand, web thickness variation is inevitable in web handling applications. Web problems such as permanent wrinkles cause thickness variations across the web. As the thicker section of the web comes in contact with the roller, the IRTMs get shorter. This results in tension peaks on the web. Higher web tension yields higher web peaks. Additionally, higher web speed also causes higher tension peaks. Determination of the ideal web tension is dependent on the yield strength (σ_y) of the electrode web, web speed and the minimum tension that causes plastic deformation on the web surface due to undulations. The web tension should be set in between the yield strength and the minimum tension limit.

The parallelism between each roll is critical. Increasing misalignment angle reduces the critical web speed. The position of each roll should be finely calibrated to avoid web instabilities. If there is a significant non-parallelism between two rolls, web tends to be taut on one portion and baggy on the other the transition region between the baggy and the taut zone is often split with a transverse fold. Adjustable web spreading solutions such as side stretching assembly are potentially useful for these cases.

High tension causes either permanent wrinkles or scratches on the web. The Air Turn avoids this problem by removing the contact between the web and the roll. Additionally, dents and air bubbles on the web surface are avoided using this solution. Besides, self-spreading effect through the use of Air Turn rolls, allow passive removal of wrinkles without using spreading equipment. Moreover, parallelism is not as critical in contactless web transport, as shear stresses due to friction between the web and roll are eliminated.

4.4. Expected Cycle Time Improvement.

Both of the proposals include upgrading the gripper linear motion to continuous motion. Even applying the same rate of acceleration and deceleration through continuous motion, the process speed can potentially increase at least by a factor of two, as the steps of the gripper are halved. This would correspond to about 33.8% cycle time improvement. Further web stability optimizations enable higher critical operating velocity. Conveying the web with 10% higher velocity would bring an additional improvement of 4.5% in the cycle time. Adding such improvements, we conclude with a cycle

time improvement of 38.3% of the electrode sheet forming process.

Table 2: Cycle time comparison

Processes	Time (s)	
	Current	Design Proposal
Die Cutting Down	0.32	0.32
Die Cutting Up	0.44	0.44
Handling On	0.55	0.495
Handling Off	0.47	0.423
Clamping Down	0.15	0.15
Clamping Up	0.47	0.47
Vacuum Gripper In	2.84	1.278
Vacuum Gripper Out	3	1.35
Vacuum On	0.2	0.2
Vacuum Off	0.2	0.2
Total	**8.64**	**5.326**

5. Outlook

All of the experiments performed on the materials were conducted outside the dry room conditions. It should be considered that commercial lithium-ion cell production takes place under the dry room conditions where humidity is minimized. Such circumstance may alter Young's modulus of the material.

During the closed-loop web experiments one of the load cells were damaged due to web tension exceeding the tension limits of the load cell. Thus, the majority of the tests were performed using one of the load cells. Eventually, the load cell was sent for replacement. Rest of the closed-loop web experiments could not be carried out in this interval as there was no bearing support on one side of the roller. The replacement arrived after three months. However, tension calibration could not be completed as the replacement tension load cell did not respond to the communication protocol.

Consequently, closed-loop experiments could not be carried out on the anode web. Besides, most of the results presented on 3.2 could not be performed on the cathode for the same reason. Thus, aluminum foil results were instead analyzed to draw conclusions. It is notable that the isotropy of the aluminum was questionable given the tensile tests. Thus, the experiments carried out with the cathode and anode electrodes could lead to different conclusions.

The copper foil has very low stiffness. It was virtually not possible to place the copper web into the experimental setups without causing severe wrinkles. Thus copper was neither in closed-loop tests nor in side stretching tests conducted. The wrinkles would alter the results of each experiment. Since these experiments could not be performed the results of the stress-strain test was also not necessary to obtain.

On closed-loop experiments, permanent wrinkles were mostly generated on the interface between the web and the adhesive tape. The tape band joins both ends of the tape. When this tape is not uniformly applied, or air was trapped between the band and the web it either leads to baggy edges or permanent wrinkle generations. Thus, the application of the tape bands was time-consuming on each closed-loop experiment.

References

[1] Schlick, Dr.T., Hertel, Dr.G., Hagemann, B., Maiser, Dr.E., Kramer, M., 2011. E-Mobility – a promising field for the future. Roland Berger Strategy Consultants.

[2] Baumeister, M., Fleischer, J., 2014. Integrated cut and place module for high productive manufacturing of lithium-ion cells. CIRP Annals 63, 5–8. https://doi.org/10.1016/j.cirp.2014.03.063

[3] Baumeister, M., 2017. Automatisierte Fertigung von Einzelblattstapeln in der Lithium-Ionen-Zellproduktion, Forschungsberichte aus dem wbk, Institut für Produktionstechnik, Karlsruher Institut für Technologie (KIT). Shaker Verlag, Aachen.

[4] Schröder, R., Glodde, A., Aydemir, M., Seliger, G., 2016. Increasing Productivity in Grasping Electrodes in Lithium-ion Battery Manufacturing. Procedia CIRP 57, 775–780. https://doi.org/10.1016/j.procir.2016.11.134

[5] Aydemir, M., Glodde, A., Mooy, R., Bach, G., 2017. Increasing productivity in assembling z-folded electrode-separator-composites for lithium-ion batteries. CIRP Annals 66, 25–28. https://doi.org/10.1016/j.cirp.2017.04.096

[6] Hawkins, W.E., 2003. The plastic film and foil Web handling guide. CRC Press, Boca Raton.

[7] Pfeiffer, J.D., 1987. Mechanics and Dynamics of Web Motion between Spans, in: Mechanics and Dynamics of Web Motion between Spans. Presented at the American Control Conference, IEEE, Minneapolis, MN, USA. https://doi.org/10.23919/ACC.1987.4789656

[8] Shelton, J.J., 1969. Lateral dynamics of a moving web. University of Oklahoma, [Norman, Okla.].

[9] Lin, C.C., Mote, C.D., 1996. Eigenvalue solutions predicting the wrinkling of rectangular webs under non-linearly distributed edge loading. Journal Of Sound And Vibration 197, 179–190.

[10] Vetter, J., Novák, P., Wagner, M.R., Veit, C., Möller, K.-C., Besenhard, J.O., Winter, M., Wohlfahrt-Mehrens, M., Vogler, C., Hammouche, A., 2005. Ageing mechanisms in lithium-ion batteries. Journal of Power Sources 147, 269–281. https://doi.org/10.1016/j.jpowsour.2005.01.006

[11] Shin, K.-H., Kwon, S.-O., 2007. The Effect of Tension on the Lateral Dynamics and Control of a Moving Web. IEEE Transactions on Industry Applications 43, 403–411. https://doi.org/10.1109/TIA.2006.889742

[12] Devitt, A.J., 2010. Method and apparatus for in-line processing and immediately sequential or simultaneous processing of flat and flexible substrates through viscous shear in thin cross section gaps for the manufacture of micro-electronic circuits or displays.